Colloids and Surfaces A: Physicochemical and Engineering Aspects 642 (2022) 128713

Contents lists available at ScienceDirect

Colloids and Surfaces A: Physicochemical and Engineering Aspects

journal homepage: www.elsevier.com/locate/colsurfa

Liquid-crystalline ordering of davydov-split aggregates of cyanine dyes

Yiping Ma, Arianna Dicce, Nitin Ramesh Reddy, Jiyu Fang *

Department of Materials Science and Engineering and Advanced Materials Processing and Analysis Center, University of Central Florida, Orlando, FL 32816, USA

HIGHLIGHTS

- Davydov-split aggregates are formed by the self-assembly of lipophilic carbocyanine dyes.
- The morphology of Davydov-split aggregates depends on the alkyl tail length of lipophilic carbocyanine dyes.
- Davydov-split aggregate vesicles and fibers show liquid-crystalline ordering.

GRAPHICAL ABSTRACT

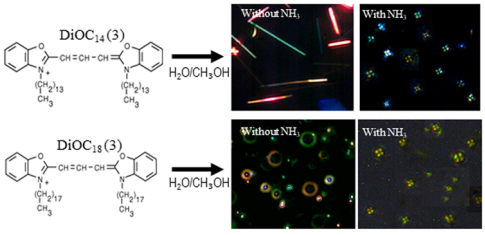

ARTICLE INFO

Keywords:
Cyanine dyes
Aggregates
Davydov splitting
Fluorescence
Liquid-crystalline order

ABSTRACT

3,3′-ditetradecyloxacarbocyanine ($DiOC_{14}(3)$) and 3,3′-Dioctadecyloxacarbocyanine ($DiOC_{18}(3)$) are lipophilic carbocyanine dyes with a conjugated polymethine backbone and two long hydrocarbon tails. In this paper, we report the formation of Davydov-split aggregates of $DiOC_{14}(3)$ and $DiOC_{18}(3)$ in methanol/water mixtures with and without ammonia, which show a blue-shifted H-band and a red-shifted J-band with respect to the monomer band in their UV–vis absorption spectra. The Davydov-split aggregates of $DiOC_{14}(3)$ show a fiber-like morphology in the absence of ammonia and a vesicle-like morphology in the presence of ammonia. While the Davydov-split aggregates of $DiOC_{18}(3)$ show a vesicle-like morphology with the different lamellarities, depending on the presence of ammonia in the methanol/water mixtures. These Davydov-split aggregates with different morphologies are birefringence when being viewed through crossed polarizers, suggesting that they have liquid-crystalline phases. The Davydov-split aggregate fibers and vesicles with liquid-crystalline phases and unique excitations are great potential for photonic applications because the liquid-crystalline order and molecular exciton are synergized.

1. Introduction

Cyanine dyes are an ionic compound composed of two heterocyclic rings linked by a conjugated backbone [1]. Due to the strong intermolecular interactions, cyanine dyes have the tendency to form J- or H-aggregates in aqueous solution, depending upon the conditions under which the aggregation occurs [2,3]. J-aggregates represent the head-to-tail arrangement of the transition dipole moments of cyanine dyes. While H-aggregates represent a face-to-face arrangement of the transition dipole moments of cyanine dyes. In some conditions, cyanine dyes form Davydov-split aggregates, in which the transition dipole moments of cyanine dyes are twisted to each other [4–6]. There has been great interest in controlling the size and morphology of these cyanine dye aggregates. For example, efforts have been made in the use of the self-assembly of amphiphilic cyanine dyes to form J- and H-aggregate ribbons and nanotubes [7–12]. In addition, inspired by the design of

* Corresponding author.
E-mail address: Jiyu.fang@ucf.edu (J. Fang).

https://doi.org/10.1016/j.colsurfa.2022.128713
Received 25 January 2022; Received in revised form 26 February 2022; Accepted 2 March 2022
Available online 7 March 2022

light-harvesting antenna in nature, templated approaches have also been developed for controlling the formation of J- and H-aggregates of cyanine dyes [13–20]. These aggregates with well-defined morphologies have potential applications for photonic devices because of their unique molecular excitons.

Liquid crystals are an ordered material, in which molecules show a long-range orientation order [21]. The supramolecular assembly through noncovalent interactions provides a new strategy for designing liquid crystals with enhanced complexity and functionality [22]. It has been shown that certain dyes can self-assemble into lyotropic chromonic liquid-crystalline phases in aqueous solution [23–25]. Although cyanine dyes have the tendency of forming J- and H-aggregates in aqueous solution, they do not typically show liquid-crystalline ordering with a few exceptions [26–28].

3,3′-Dioctadecyloxacarbocyanine ($DiOC_{18}(3)$) and 3,3′-ditetradecyloxacarbocyanine ($DiOC_{14}(3)$) are lipophilic cyanine dyes. It has been shown that $DiOC_{18}(3)$ can form Langmuir monolayers at the air-water interface [29]. The H-aggregates formed in the liquid condensed phase of the Langmuir monolayers are fluorescent due to the twisted stacking of $DiOC_{18}(3)$ molecules [30]. However, the aggregation behavior of these lipophilic cyanine dyes in solution is largely unexplored. In this paper, we show that $DiOC_{14}(3)$ and $DiOC_{18}(3)$ in methanol/water mixtures with and without ammonia form Davydov-split aggregates, which show a blue-shifted H-band and a red-shifted J-band with respect to the monomer band in their absorption spectra. The twisted angle of the transition dipole moments of $DiOC_{14}(3)$ and $DiOC_{18}(3)$ in the Davydov-split aggregates was estimated from their absorption spectra. Davydov-split aggregates are fluorescent and show liquid-crystalline phases. The morphology of the Davydov-split aggregates depends on the experimental condition under which the aggregation of $DiOC_{14}(3)$ and $DiOC_{18}(3)$ occurs.

2. Experimental section

2.1. Materials

3,3′-ditetradecyloxacarbocyanine ($DiOC_{14}(3)$), 3,3′-Dioctadecyloxacarbocyanine ($DiOC_{18}(3)$), sodium chloride (NaCl), and sodium hydroxide (NaOH) were purchased from Sigma-Aldrich and used without purification. Deionized water (18 MΩ cm, pH 5.7) was obtained from Easypure II system. Methanol and ammonia solution were from Sigma-Aldrich. Carbon-coated copper grids were from SPI supplies.

2.2. Formation of Davydov-split aggregates

$DiOC_{14}(3)$ and $DiOC_{18}(3)$ were dissolved in methanol at 55 °C for forming stock solutions, respectively. The stock solution was then mixed with water at the equal volume ratio with and without ammonia, sodium chloride (NaCl), and sodium hydroxide (NaOH). The mixed solution was sonicated at ~50 °C in an ultrasonic bath (Branson 1510, Branson Ultrasonics Co.) for 5 min and then cooled to room temperature. After the mixed solution was aged at room temperature, a color change was observed. This suggested that the aggregation of $DiOC_{14}(3)$ and $DiOC_{18}(3)$ took place. The aggregate solution was stored in the dark when not in use.

2.3. Characterizations

Zeta-potential measurements were carried out with a Zetasizer Nano ZS90 (Malvern Instruments Inc.) at a cell driven voltage of 30 V. The absorption spectra of aggregation solution were measured with a Cary 400 UV–vis spectrophotometer. Fluorescence spectra were measured at the synchronous mode with $\Delta = 40$ nm using Jasco FP-6500 spectrofluorometer. The optical and fluorescent microscopy images of aggregates were taken with an Olympus BX40 microscope with a hot stage and a Cytation 5 imaging reader equipped with a Xenon flash lamp and a DAPI filter cube, respectively. For the polarizing optical microscopy measurements, the optics was adjusted to complete extinction before samples were placed on the stage. The optical microscopy images were captured by using a digital camera (C2020 Zoom, Olympus) mounted on the microscope. Transmission electron microscopy (TEM) measurements were carried out with a JEOL TEM 1011 at an accelerating voltage of 100 kV, in which a drop of aggregation solution was dried on carbon-coated copper grids.

3. Results and discussion

The chemical structure of $DiOC_{14}(3)$ and $DiOC_{18}(3)$ is shown in Fig. 1a. Both dyes have the same conjugated polymethine backbone, but different lengths of alkyl tails. In methanol, the UV–vis absorption spectrum of $DiOC_{14}(3)$ and $DiOC_{18}(3)$ was characterized by a major monomer band at 485 nm and a shoulder short-wavelength shoulder band at 457 nm (Fig. 1b). The appearance of the shoulder band could be due to the formation of dimers [31]. $DiOC_{14}(3)$ with the concentration of 0.15 mM in the methanol/water mixture (1:1, v/v) showed a strong monomer band with a shoulder at 510 nm and a weak H-band at 387 nm after the solution was aged for 1 h (Fig. 2a). In this case, $DiOC_{14}(3)$ formed vesicle-like aggregates (Fig. 2b), which showed no birefringence when being viewed under a polarizing optical microscope. This result suggested that the vesicle-like aggregates had a liquid-like phase. After 24 h aging, the intensity of the H-band at 387 nm significantly increased. At the same time, a J-band at 501 nm was observed (Fig. 2a). The intensity of the J-band was slightly higher than that of the H-band. The change of the UV–vis absorption spectra over time was a result of the rearrangement of $DiOC_{14}(3)$ molecules in aggregates. The appearance of both the J-band and the H-band in the UV-Vis absorption spectra suggested that $DiOC_{14}(3)$ molecules formed Davydov-split aggregates, in which the transition dipole moments of $DiOC_{14}(3)$ molecules are twisted to each other. Interestingly, the Davydov-split aggregates of $DiOC_{14}(3)$ molecules showed a fiber-like structure with birefringence when being viewed under a polarizing optical microscope (Fig. 2c), suggesting that the $DiOC_{14}(3)$ molecules had a liquid-crystalline phase in the Davydov-split aggregate fibers. The twisted arrangement of $DiOC_{14}(3)$ molecules in the Davydov-split aggregate fibers allows optical transitions to both the higher (E_1) and lower (E_2) excited states, producing both the blue-shifted H-band and the red-shifted J-band in absorption spectra (Fig. 2d). The twisted angle (θ) of the transition moments of molecules in Davydov-split aggregates could be estimated from the equation [32,33]: $tan^2\frac{\theta}{2} = \frac{A_{J-band}}{A_{H-band}}$, where $A_{J\text{-band}}$ and $A_{H\text{-band}}$ were the oscillation strength of the J-band and the H-band, respectively. The ratio of $A_{J\text{-band}}/A_{H\text{-band}}$ was proportional to the ratio of the areas under the H-band and the J-band in adsorption spectra. Due to the overlap of the H-band and J-band of the Davydov-split aggregate fibers, we estimated the twisted angles (θ) of the transition moments of $DiOC_{14}(3)$ molecules from the intensity ratio of the H-band and the J-band to be ~ 84°. Recently, the essential state model was developed for the understanding of the Davydov-split aggregates of squaraine dimers, which predicted that the H-band was dominant when the twisted angel of the squaraine dimers was close ~ 0°. The J-band became dominant when the twisted angle of the squaraine dimers was close to 180°. Both the intense J-band and the H-band appeared when the twisted angel of the squaraine dimers was in the range from 180° to 0° [34], which was reasonable in the agreement with our results.

The UV–vis absorption spectra of 0.25 mM $DiOC_{14}(3)$ in the methanol/water mixture (1:1, v/v) were near identical to that of 0.15 mM $DiOC_{14}(3)$ except the relative intensity of the H- and J-band after the solution was aged for 24 h (Fig. 3a). In this case, the intensity of the H-band at 387 nm was slightly higher than that the J-band at 501 nm. The Davydov-split aggregates formed from 0.25 mM $DiOC_{14}(3)$ also showed a fiber-like structure (Fig. 3b). The Davydov-split aggregate fibers changed birefringence when they were rotated in the plane (Fig. 3c),

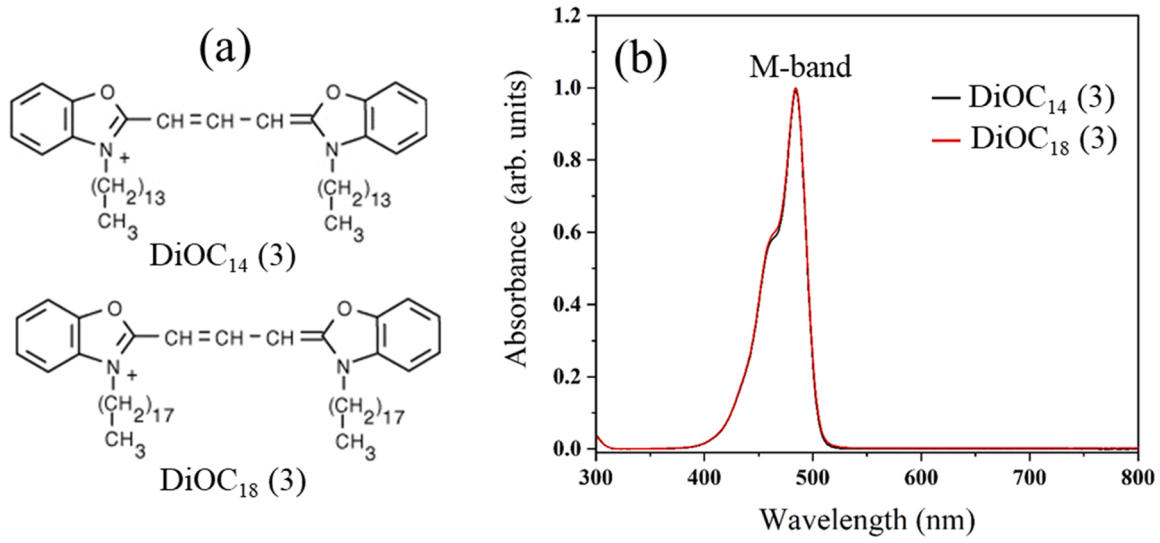

Fig. 1. (a) Chemical structure of $DiOC_{14}(3)$ and $DiOC_{18}(3)$. (b) UV-Vis absorption spectra of 0.25 mM $DiOC_{14}(3)$ and $DiOC_{18}(3)$ in methanol.

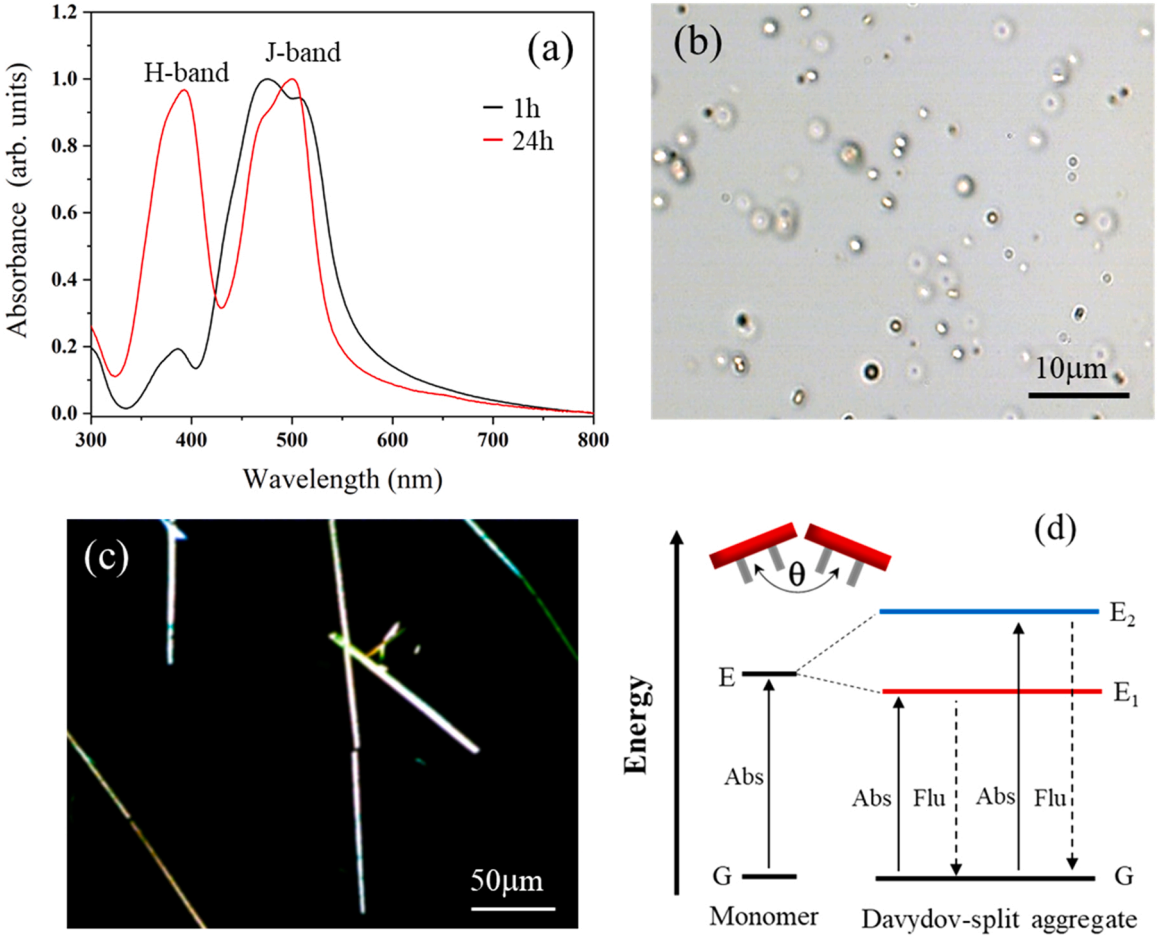

Fig. 2. (a) UV-Vis absorption spectra of 0.15 mM $DiOC_{14}(3)$ in the methanol/water mixture (1:1, v/v) after being aged for 1 h and 24 h. (b) Optical microscopy image of $DiOC_{14}(3)$ vesicles formed after being aged for 1 h. (c) Polarizing microscopy image of Davydov-split aggregate fibers formed after being aged for 24 h. (d) Schematic energy diagram and optical transition of monomers and Davydov-split aggregates. Schematic representation of a twisted arrangement of $DiOC_{14}(3)$ molecules was inserted in d.

which could point on the presence of liquid-crystalline structures. The liquid-crystalline phase was also observed in pure H- or J-aggregate fibers [35] and J-aggregate sheets [36] of other dyes. The twisted angles (θ) of the transition moments of $DiOC_{14}(3)$ molecules in the Davydov-split aggregate fibers was estimated to be ~ 83° from the intensity ratio of the H-band and the J-band. The Davydov-split aggregate

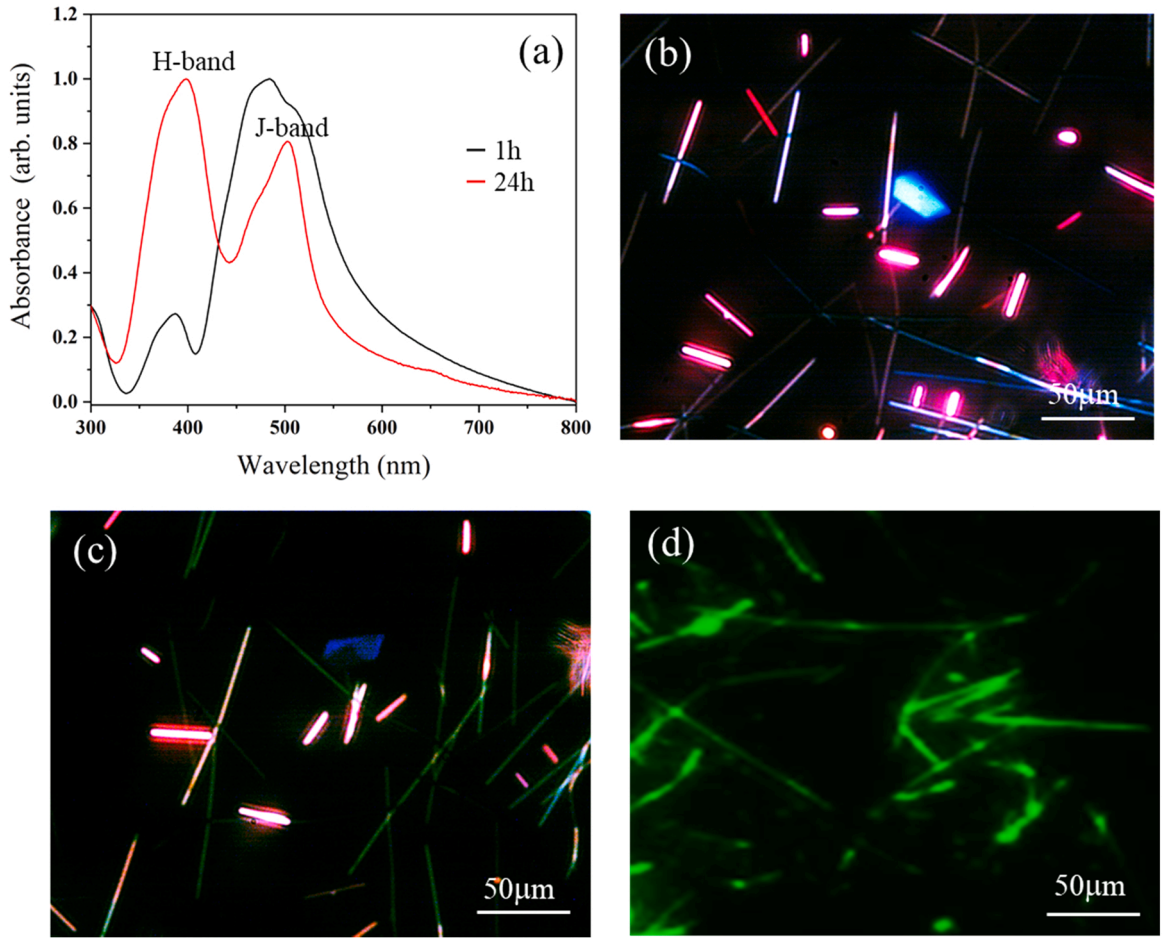

Fig. 3. (a) UV-Vis absorption spectra of 0.25 mM $DiOC_{14}(3)$ in the methanol/water mixture (1:1, v/v) after being aged for 1 h and 24 h. (b, c) Polarizing optical microscopy images of Davydov-split aggregate fibers formed after being aged for 24 h. The images were taken when the fibers were rotated. (d) Fluorescence microscopy image of Davydov-split aggregate fibers formed after being aged for 24 h.

fibers were fluorescent (Fig. 3d), in which some fluorescent vesicles were observed to connect with the fibers. Thus, we speculated that the crystallization of $DiOC_{14}(3)$ molecules led to the vesicle-to-fiber transition. The transition was also observed in the aggregation process of other dyes [37] and surfactants [38–40]. There was no Davydov-split aggregate fiber observed when the concentration of $DiOC_{14}(3)$ in the methanol/water mixture (1:1, v/v) was reduced to 0.07 mM.

After the addition of 1% ammonia in the methanol/water mixture (1:1, v/v), the positions of the H- and J-bands of 0.25 mM $DiOC_{14}(3)$ slightly red-shifted with respect to that in the absence of 1% ammonia

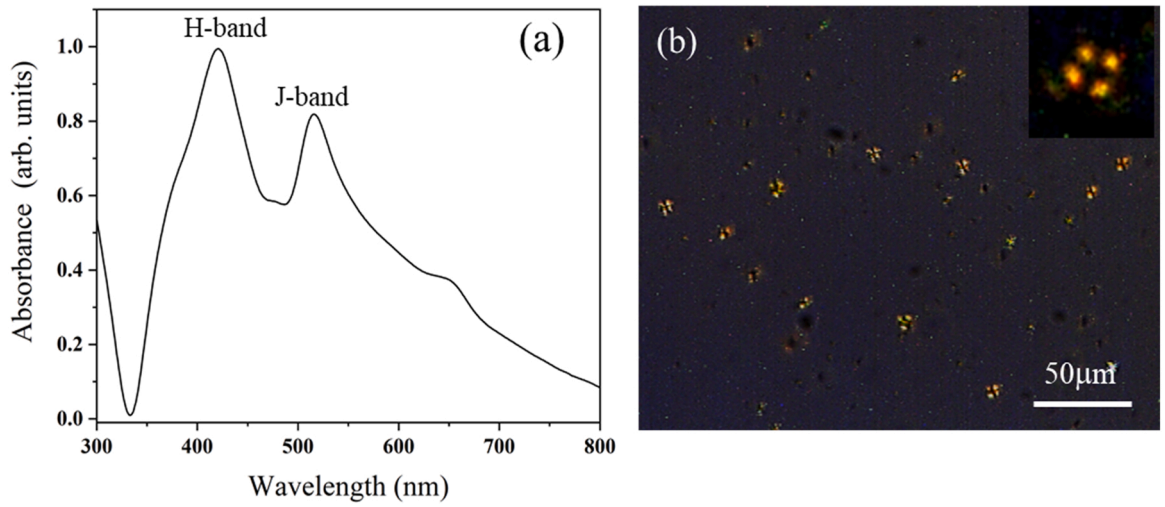

Fig. 4. (a) UV-Vis absorption spectrum of 0.25 mM $DiOC_{14}(3)$ in the methanol/water mixture (1:1, v/v) with 1% ammonia after being aged for 24 h. (b) Polarizing optical microscopy image of Davydov-split aggregate vesicles. An enlarged polarizing microscopy image of a vesicle was inserted in b.

(Fig. 4a). In this case, the intensity of the J-band at 410 nm is slightly higher than that of the H-band at 508 nm. The Davydov-split aggregates of $DiOC_{14}(3)$ in the presence of 1% ammonia showed a vesicle-like structure with a birefringent Maltese-cross pattern (Fig. 4b), suggesting that the vesicle had a liquid-crystalline phase. There was no vesicle-to-fiber transition observed even after several day aging. The twisted angles (θ) of the transition moments of $DiOC_{14}(3)$ molecules in Davydov-split aggregate vesicles were estimated to be ~ 84° from the relative intensity ratio of the H-band and the J-band.

The aggregation of $DiOC_{14}(3)$ molecules in solution is driven by hydrophobic interaction, electrostatic interaction, and π-π stacking. The balance of these interactions is responsible for the formation of Davydov-split aggregates. It was proposed that the hydrophobic interaction of the alkyl tails of lipophilic cyanine dyes was a main driving force to cause the twisting of the transition moments of the dyes within the Langmuir monolayers at the air-water interface [29,30]. Ammonia is a weak base, which reacts with water to form ammonium ions (NH_4^+) and hydroxide ions (OH^-). In the methanol/water mixture with ammonia, OH^- ions might screen the charge of $DiOC_{14}(3)$ molecules to reduce their electrostatic repulsion. Due to the charge screening of $DiOC_{14}(3)$ molecules by OH^- ions, the π–π stacking of $DiOC_{14}(3)$ molecules increased, which might lead to the formation of liquid-crystalline phase in Davydov-split aggregate vesicles.

The UV–vis absorption spectrum of both 0.15 mM and 0.25 mM $DiOC_{18}(3)$ in the methanol/water mixture (1:1, v/v) also showed Davydov splitting with a blue-shifted H-band at 384 nm and a red-shifted J-band at 502 nm (Fig. 5a). The diameter of Davydov-split aggregate vesicles formed by 0.15 mM $DiOC_{18}(3)$ was typically smaller than 2.0 μm (Fig. 5b). While the Davydov-split aggregate vesicles formed by 0.25 mM $DiOC_{18}(3)$ showed the diameter in the range from 1.0 μm to 7.0 μm (Fig. 5c). The twisted angle (θ) of the transition moments of $DiOC_{18}(3)$ molecules was estimated from the relative intensity of the H-band and the J-band to be ~ 83° in the Davydov-split aggregate vesicles formed by 0.15 mM $DiOC_{18}(3)$ and ~ 84° in the Davydov-split aggregate vesicles formed by .25 mM $DiOC_{18}(3)$. All the Davydov-split aggregate vesicles showed birefringence in their peripheral regions (Fig. 5b and c). TEM images revealed the presence of nanosized Davydov-split aggregate vesicles as well (Fig. 5d), which deformed after being dried on substrates. The deformed vesicles showed a donut shape.

The Davydov-split aggregate vesicles of $DiOC_{18}(3)$ showed a weak fluorescence emission at 449 nm and a strong fluorescence emission at 553 nm (Fig. 6a). The Stokes shift of the strong fluorescence emission with respect to the J-band was 51 nm. For Davydov-split aggregates, the exciton band splits into two energy states, in which the fluorescence from both the higher and lower exciton states become possible due to the twisting of their transition moments (Fig. 2d). The weak fluorescence emission at 449 nm should be from the higher energy state (E_2), while the strong fluorescence emission at 553 nm is from the lower energy state (E_1). The Davydov-split aggregate vesicles showed a fluorescence from the peripheral region of the vesicles (Fig. 6b). The results from polarizing and fluorescence microscopy images suggested that the

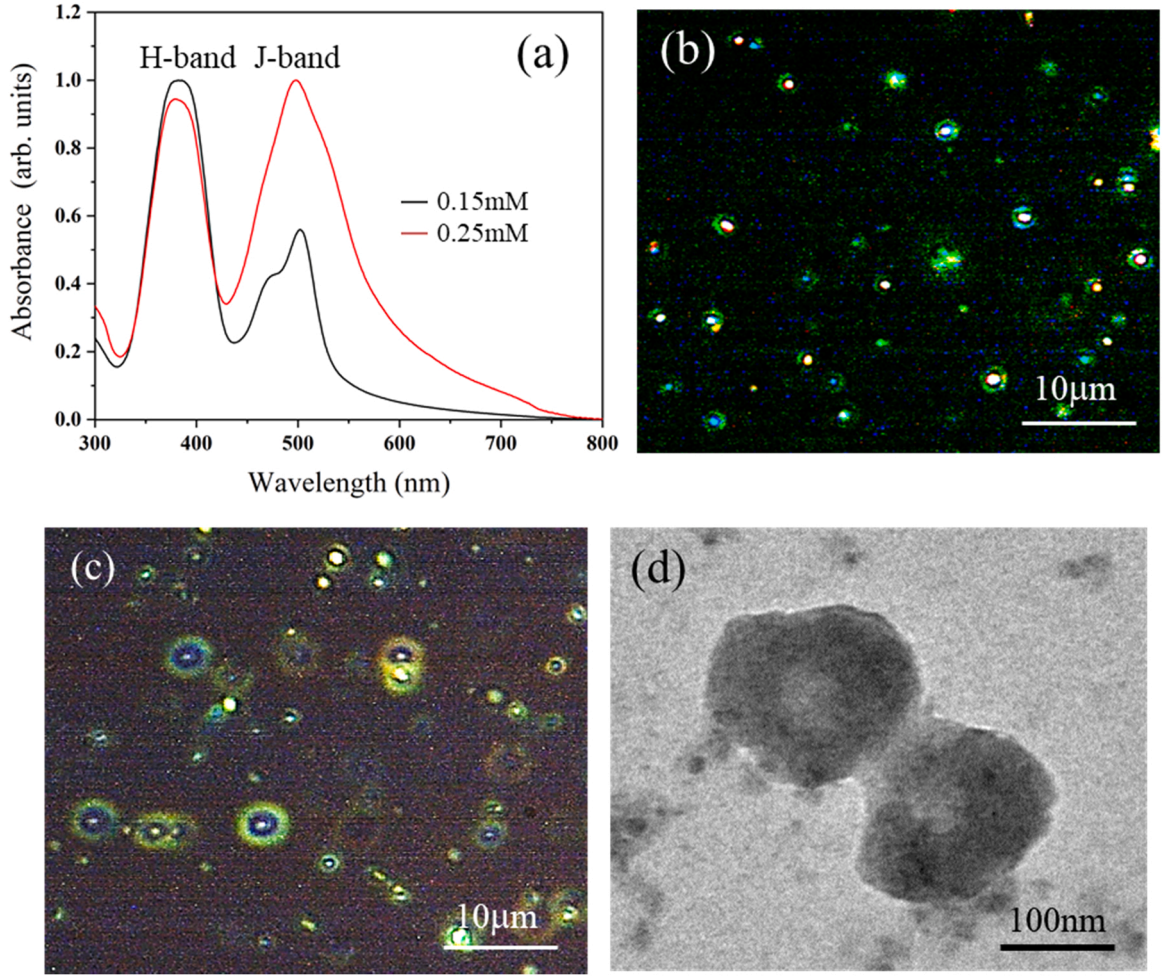

Fig. 5. (a) UV-Vis absorption spectra of 0.15 mM and 0.25 mM $DiOC_{18}(3)$ in the methanol/water mixture (1:1, v/v) after being aged for 24 h. Polarizing microscopy images of Davydov-split aggregate vesicles formed by 0.15 mM (b) and 0.25 mM $DiOC_{18}(3)$ (c) at room temperature. (d) TEM Davydov-split aggregate vesicles formed by 0.25 mM $DiOC_{18}(3)$.

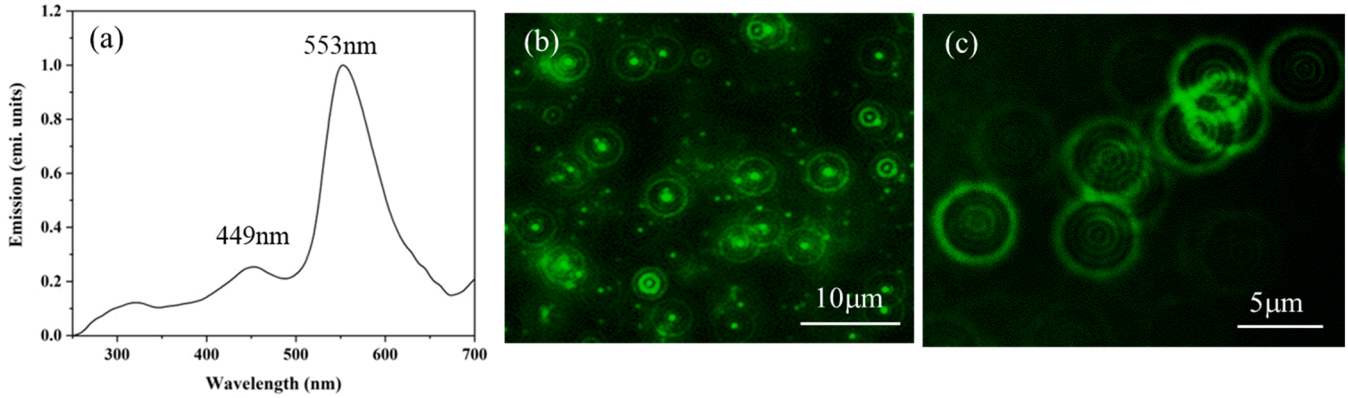

Fig. 6. (a) Fluorescence emission spectrum of Davydov-split aggregate vesicles formed by 0.25 mM $DiOC_{18}(3)$ in the methanol/water mixture (1:1, v/v) after being aged for 24 h. (b, c) Fluorescence microscopy images of Davydov-split aggregate vesicles formed in the methanol/water mixture (1:1, v/v) after being aged for 24 h.

$DiOC_{18}(3)$ molecules arranged in the peripheral region the surface of the vesicles formed a liquid-crystalline phase. In this case, there was no vesicle-to-fiber transition observed even when the liquid-crystalline vesicles were in contact with each other (Fig. 6c).

The addition of 1% ammonia in the methanol/water mixture (1:1, v/v) caused the slight red-shift of both the H-band and J-band of Davydov-split aggregate vesicles with respect to that in the absence of ammonia (Fig. 7a). In this case, the Davydov splitting was characterized by a H-band at 420 nm and a J-band at 516 nm. The twisted angle (θ) of the transition moments of $DiOC_{18}(3)$ in Davydov-split aggregate vesicles was estimated to be 79°. The Davydov-split aggregates showed a weak fluorescence emission at 478 nm and a strong fluorescence emission at 563 nm (Fig. 7a). The strong fluorescence emission had a Stokes shift of 47 nm with respect to the J-band. When being viewed with a polarizing optical microscope, the Davydov split aggregate vesicles of $DiOC_{18}(3)$ showed a Maltese-cross pattern of light extinction (Fig. 7b). The Maltese-cross pattern of light extinction was also observed for the multi-lamellar vesicles of lipids in gel phases [41,42], in which the hydrophobic tails of lipids were oriented along the radial direction of the vesicles. The Davydov-split aggregates of $DiOC_{18}(3)$ showed relatively uniform

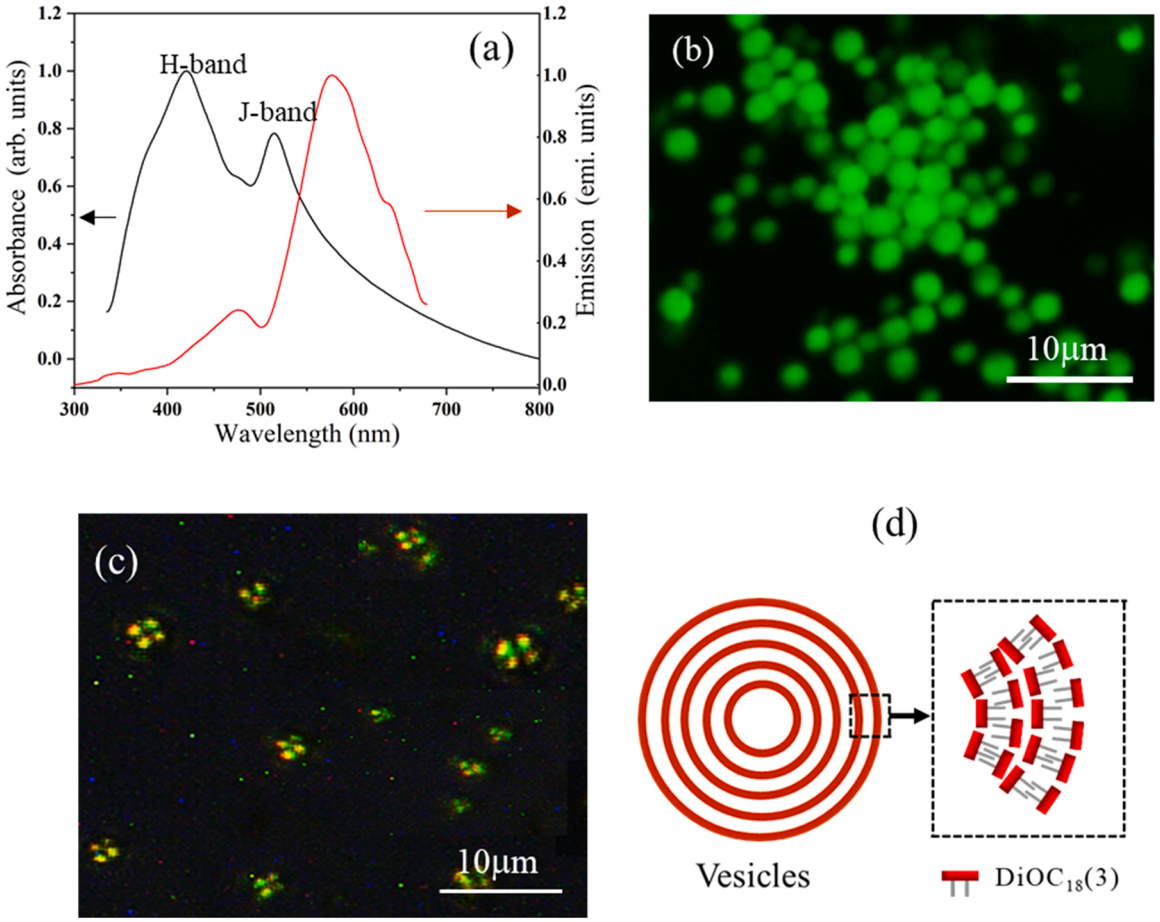

Fig. 7. UV-Vis absorption and fluorescence emission spectra of Davydov-split aggregate vesicles formed by 0.25 mM $DiOC_{18}(3)$ the methanol/water mixture (1:1, v/v) with 1% of ammonia. Fluorescence (b) and polarizing (c) optical microscopy images of Davydov-split aggregate vesicles. (d) Schematic of multi-lamellar vesicles of $DiOC_{18}(3)$.

fluorescence (Fig. 7c). The zeta potential of Davydov-split aggregate vesicles of $DiOC_{18}(3)$ was ~ 17.4 eV, suggesting that the surface of the vesicles was terminated by the cationic polymethine backbone of $DiOC_{18}(3)$. Based on the amphiphilic nature of $DiOC_{18}(3)$ together with the appearance of the birefringence Maltese-cross pattern, we concluded that $DiOC_{18}(3)$ formed a multi-lamellar liquid-crystalline phase, in which the alkyl tail of $DiOC_{18}(3)$ was radially oriented within the vesicles (Fig. 7d).

The appearance of the birefringence and fluorescent rings in the peripheral region of Davydov-split aggregate vesicles of $DiOC_{18}(3)$ in the absence of ammonia (Fig. 5b and Fig. 6b) might suggest that the degree of lamellarity of the vesicles was low. In the presence of ammonia, the charge of $DiOC_{18}(3)$ molecules was screened by OH^- ions. In this case, Davydov- split aggregate vesicles of $DiOC_{18}(3)$ showed a uniform fluorescence and a birefringence Maltese-cross pattern, suggesting that the degree of lamellarity of the vesicles was high. It was reported that charged lipids promoted the unilamellarity in vesicles, while neutral lipids favored the multi-lamellarity in vesicles [43,44]. Our results were reasonable in the agreement with the relationship of the degree of lamellarity of lipid vesicles with the charge of lipids.

Finally, we measured the UV–vis absorption spectra of 0.25 mM $DiOC_{18}(3)$ in the methanol/water mixture (1:1, v/v) after the addition of 3.25 mM NaCl and 3.25 mM NaOH, respectively. The position of the H-band and the J-band of Davydov-split aggregate vesicles remained unchanged after the addition of NaCl (Fig. 8a). In this case, the Davydov-split aggregate vesicles of $DiOC_{18}(3)$ showed a birefringence ring (Fig. 8b). On the other hand, the position of the H-band and the J-band of 0.25 mM $DiOC_{18}(3)$ was red-shifted after the addition of NaOH (Fig. 8c). In this case, The Davydov-split aggregate vesicles of $DiOC_{18}(3)$ showed a birefringence Maltese cross pattern (Fig. 8d). These results might suggest that Cl^- ions were not efficient in screening the charge of $DiOC_{18}(3)$ molecules, compared to OH^- ions.

4. Conclusions

We have shown that lipophilic $DiOC_{14}(3)$ and $DiOC_{18}(3)$ in the methanol/water mixture with/without ammonia can form Davydov-split aggregates, which show a blue-shifted H-band and a red-shifted J-band with respect to the monomer band in their UV–vis absorption spectra. The Davydov-split aggregates of $DiOC_{14}(3)$ show a fiber-like morphology in the absence of ammonia and a vesicle-like morphology in the presence of ammonia. While the Davydov-split aggregates of $DiOC_{18}(3)$ show a vesicle-like morphology with the low degree of lamellarity in the absence of ammonia and the high degree of lamellarity in the presence of ammonia. The Davydov-split aggregate fibers and vesicles show liquid-crystalline phases, which are great potential for designing artificial light-harvesting and photonic devices.

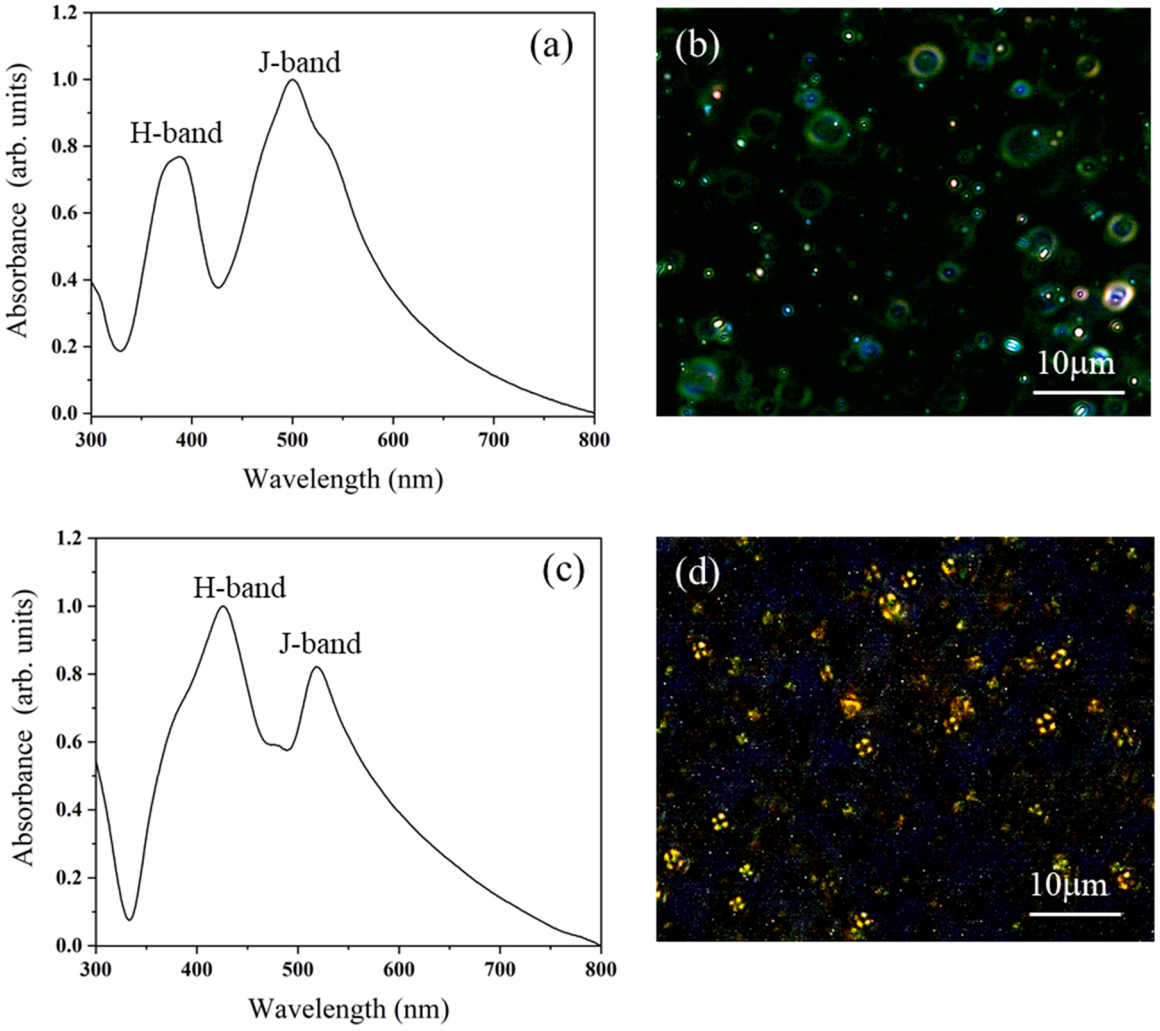

Fig. 8. (a) UV-Vis absorption spectrum and (b) polarizing optical microscopy image of Davydov-split aggregate vesicles of $DiOC_{18}(3)$ formed in the methanol/water mixture (1:1, v/v) with 2.3 mM NaCl. (c) UV-Vis absorption spectrum and (d) polarizing optical microscopy image of Davydov-split aggregate vesicles of $DiOC_{18}(3)$ formed in the methanol/water mixture (1:1, v/v) with 2.3 mM NaOH.

CRediT authorship contribution statement

Yiping Ma: Data curation, Validation, Methodology. **Arianna Dicce:** Validation. **Nitin Ramesh Reddy**: Validation. **Jiyu Fang**: Conceptualization, Supervision, Writing.

Declaration of Competing Interest

The authors declare that they have no known competing financial interests or personal relationships that could have appeared to influence the work reported in this paper.

Acknowledgments

This work was supported by the USA National Science Foundation (CBET 1803690).

References

[1] A. Mishra, R.K. Behera, P.K. Behera, B.K. Mishra, G.B. Behera, Cyanines during the 1990s: a review, Chem. Rev. 100 (2000) 1973–2012.
[2] F. Würthner, T.E. Kaiser, C.R. Saha-Möller, J-Aggregates: from serendipitous discovery to supramolecular engineering of functional dye, Mater. Angew. Chem. Int. Ed. 50 (2011) 3376–3410.
[3] F.C. Spano, The spectral signatures of frenkel polarons in H- and J-aggregates, Acc. Chem. Res. 43 (2010) 429–439.
[4] U. DeRossi, S. Dahne, S.C.J. Meskers, H.P.J.M. Dekkers, Spontaneous formation of chirality in J-aggregates showing davydov splitting, Angew. Chem. Int. Ed. 35 (1996) 760–763.
[5] B.L. Cannon, L.K. Patten, D.L. Kellis, P.H. Davis, J. Lee, E. Graugnard, B. Yurke, W. B. Knowlton, Large Davydov splitting and strong fluorescence suppression: an investigation of exciton delocalization in DNA-templated holliday junction dye aggregates, J. Phys. Chem. A 122 (2018) 2086–2095.
[6] N.R. Reddy, S. Rhodes, Y. Ma, J.Y. Fang, Davydov split aggregates of cyanine dyes on self-assembled nanotubes, Langmuir 36 (2020) 13649–13655.
[7] H. von Berlepsch, C. Böttcher, A. Ouart, C. Burger, S. Dähne, S. Kirstein, Supramolecular structures of J-aggregates of carbocyanine dyes in solution, J. Phys. Chem. B 104 (2000) 5255–5262.
[8] E. Lang, A. Sorokin, M. Drechsler, Y.V. Malyukin, J. Köhler, Optical spectroscopy on individual amphi-PIC J-aggregates, Nano Lett. 5 (2005) 2635–2640.
[9] D.M. Eisele, W. Cone, E.A. Bloemsma, S.M. Vlaming, C.G.F. vanderKwaak, R. J. Silbey, M.G. Bawendi, J. Knoester, J.P. Rabe, D.A. Vanden Bout, Utilizing redox-chemistry to elucidate the nature of exciton transitions in supramolecular dye nanotubes, Nat. Chem. 4 (2012) 655–662.
[10] K.A. Clark, E.L. Krueger, D.A. Vanden Bout, Direct measurement of energy migration in supramolecular carbocyanine dye nanotubes, J. Phys. Chem. Lett. 5 (2014) 2274–2282.
[11] D.M. Eisele, D.H. Arias, X. Fu, E.A. Bloemsma, C.P. Steiner, R.A. Jensen, P. Rebentrost, H. Eisele, A. Tokmakoff, S. Lloyd, N.A. Nelson, D. Nicastro, J. Knoester, M.G. Bawendi, Robust excitons inhabit soft supramolecular nanotubes, Proc. Natl. Acad. Sci. U. S. A. 111 (2014) E3367–E3375.
[12] B. Kriete, B.S. Bondarenko, V.R. Jumde, L.E. Franken, A.J. Minnaard, T.L. C. Jansen, J. Knoester, M.S. Pshenichnikov, Steering self-assembly of amphiphilic molecular nanostructures via halogen exchange, J. Phys. Chem. Lett. 8 (2017) 2895–2901.
[13] W. Wang, G.L. Silva, B.A. Armitage, DNA-templated formation of a helical cyanine dye J-aggregate, J. Am. Chem. Soc. 122 (2000) 9977–9986.
[14] T. Sagawa, H. Tobata, H. Ihara, Exciton interactions in cyanine dye–hyaluronic acid (HA) complex: reversible and biphasic molecular switching of chromophores induced by random coil-to-double-helix phase transition of HA, Chem. Commun. 18 (2004) 2090–2091.
[15] O.-K. Kim, J. Je, G. Jernigan, L. Buckley, D. Whitten, Super-helix formation induced by cyanine J-aggregates onto random-coil carboxymethyl amylose as template, J. Am. Chem. Soc. 128 (2006) 510–516.
[16] Q. Yang, J. Xiang, Q. Li, W. Yan, Q. Zhou, Y. Tang, G. Xu, Chiral transformation of cyanine dye aggregates induced by small peptides, J. Phys. Chem. B 112 (2008) 8783–8787.
[17] N. Ryu, Y. Okazaki, E. Pouget, M. Takafuji, S. Nagaoka, H. Ihara, R. Oda, Fluorescence emission originated from the H-aggregated cyanine dye with chiral gemini surfactant assemblies having a narrow absorption band and a remarkably large stokes shift, Chem. Commun. 53 (2017) 8870–8875.
[18] S. Rhodes, W. Liang, E. Shteinberg, J.Y. Fang, Formation of spherulitic J-aggregates from the coassembly of lithocholic acid and cyanine Dye, J. Phys. Chem. Lett. 8 (2017) 4504–4509.
[19] S. Rhodes, W. Liang, X. Wang, N.R. Reddy, J.Y. Fang, Transition from H-aggregate nanotubes to J-aggregate nanoribbons, J. Phys. Chem. C. 124 (124) (2020) 11722–11729.
[20] A. Kamalakshan, R. Ansilda, S. Mandal, Nanotube template-directed formation of strongly coupled dye aggregates with tunable exciton fluorescence controlled by switching between J- and H-Type electronic coupling, J. Phys. Chem. B 125 (2021) 7447–7455.
[21] P.G. de Gennes, J. Prost, The Physics of Liquid Crystals, Clarendon Press, 1993.
[22] T. Kato, N. Mizoshita, K. Kishimoto, Functional liquid-crystalline assemblies: self-organized soft materials, Angew. Chem. Int. Ed. 45 (2006) 38–68.
[23] A. Yu, N. Nastishin, T. Liu, V. Schneider, R. Nazarenko, S.V. Shiyanovskii, O. D. Lavrentovich, Optical characterization of the nematic lyotropic chromonic liquid crystals: light absorption, birefringence, and scalar order parameter, Phys. Rev. E 72 (2005), 041711.
[24] M.R. Tomasik, P.J. Collings, Aggregation behavior and chromonic liquid crystal phase of a dye derived from naphthalenecarboxylic acid, J. Phys. Chem. B 112 (2008) 9883–9889.
[25] J. Lydon, Chromonic review, J. Mater. Chem. 20 (2010) 10071–10099.
[26] W.J. Harrison, D.L. Mateer, G.J.T. Tiddy, Liquid-crystalline J-aggregates formed by aqueous ionic cyanine dyes, J. Phys. Chem. 100 (1996) 2310–2321.
[27] H. Yao, T. Isohashi, K. Kimura, Electrolyte-induced mesoscopic aggregation of thiacarbocyanine dye in aqueous solution: counterion size specificity, J. Phys. Chem. B 111 (2007) 7176–7183.
[28] S. Hecht, B. Soberats, P. Leowanawat, M. Lehmann, F. Würthner, A columnar liquid-crystal phase formed by hydrogen-bonded perylene bisimide J-aggregates, Angew. Chem. Int. Ed. 56 (2017) 2162–2165.
[29] Y. Miyauchia, R. Yukutakea, K. Tsuchidaa, Y. Umemuraa, A. Tsukamotoa, T. Suzuki, Observation by optical second harmonic generation of the mean tilt angle of cyanine dyes during compression with a phase transition in a Langmuir-Blodgett trough, Chem. Phys. 517 (2019) 85–90.
[30] S. Chakraborty, P. Debnath, D. Dey, D. Bhattacharjee, S.A. Hussain, Formation of fluorescent H-aggregates of a cyanine dye in ultrathinfilm and its effect on energy transfer, J. Photochem. Photobio. A 293 (2014) 57–64.
[31] A.K. Chibisov, G.V. Zakharova, H. Görner, Photoprocesses in dimers of thiacarbocyanines, Phys. Chem. Chem. Phys. 1 (1999) 1455–1460.
[32] S. Kirstein, H. Möhwald, Exciton band structures in 2D aggregates of cyanine dyes, Adv. Mater. 7 (1995) 460–463.
[33] T.N. Tkacheva, S.L. Yefimova, V.K. Klochkov, I.A. Borovoy, Y.V. Malyukin, Spectroscopic study of ordered hybrid complexes formation between dye aggregates and ReVO4:Eu3+(Re = Y, Gd, La) nanoparticles, J. Mol. Liq. 199 (2014) 244–250.
[34] C. Zhong, D. Bialas, C.J. Collison, C.F. Spano, Davydov splitting in squaraine dimers, J. Phys. Chem. C 123 (2019) 18734–18745.
[35] H. Yao, K. Domoto, T. Isohashi, K. Kimura, In situ detection of birefringent mesoscopic H and J aggregates of thiacarbocyanine dye in solution, Langmuir 21 (2005) 1067–1073.
[36] V.V. Prokhorov, S.I. Pozin, D.A. Lypenko, O.M. Perelygina, E.I. Maltsev, A. V. Vannikov, Molecular arrangements in polymorphous monolayer structures of carbocyanine dye J-aggregates, Chem. Phys. Lett. 535 (2012) 94–99.
[37] N.R. Reddy, M. Aubin, K. Kushima, J.Y. Fang, Fluorescent H-aggregate vesicles and tubes and their applications as light-harvesting antenna, J. Phys. Chem. B 125 (2021) 7911–7918.
[38] V.H.S. Tellini, A. Jover, F. Meijide, J.V. Tato, L. Galantini, N.V. Pavel, Supramolecular structures generated by a p-tert-butylphenyl-amide derivative of cholic acid: from vesicles to molecular tubes, Adv. Mater. 19 (2007) 1752–1756.
[39] W. Liang, X. He, N.R. Reddy, Y. Bai, L. An, J.Y. Fang, Morphology transformation of supramolecular structures in aqueous mixtures of two oppositely charged amphiphiles, Langmuir 35 (2019) 9004–9010.
[40] Q. Li, X. Chen, X. Yue, D. Huang, X. Wang, Construction and transformation of stimuli-responsive vesicles from the ferrocene derivative supramolecular amphiphiles, Colloids Surf. A. 409 (2012) 98–104.
[41] K. Mishima, K. Satoh, T. Ogihara, Optical birefringence of phosphatidylcholine liposomes in gel phases, Biochim. Biophys. Acta 898 (1987) 231–238.
[42] T. Haller, A. Cerrada, K. Pfaller, P. Braubach, E. Felder, Polarized light microscopy reveals physiological and drug-induced changes in surfactant membrane assembly in alveolar type II pneumocytes, Biochim. Biophys. Acta 2018 (1860) 1152–1161.
[43] J. Drazenovic, H. Wang, K. Roth, J. Zhang, S. Ahmed, Y. Chen, G. Bothun, S. L. Wunder, Effect of lamellarity and size on calorimetric phase transitions in single component phosphatidylcholine vesicles, Biochim. Biophys. Acta 2015 (1848) 532–543.
[44] M. Chiba, M. Miyazaki, S. Ishiwata, Quantitative analysis of the lamellarity of giant liposomes prepared by the inverted emulsion method, Biophys. J. 107 (2014) 346–354.